

Temperature Dependence of Hydrogen-Bond Dynamics in Acetic Acid–Water Solutions

Francesco D'Amico,* Filippo Bencivenga, Alessandro Gessini, and Claudio Masciovecchio

Sincrotrone Trieste, Strada Statale 14 km 163.5, Area Science Park, I-34149 Trieste, Italy

Received: April 26, 2010; Revised Manuscript Received: July 8, 2010

An inelastic UV scattering experiment has been carried out on acetic acid–water solutions as a function of temperature and concentration. The analysis of experimental data indicates the presence of a crossover temperature ($T_c \approx 325 \pm 10$ K). Above T_c , the energy of hydrogen bonds responsible for water–acetic acid and acetic acid–acetic acid interactions is strongly reduced. This leads to a reduction in the average number of water molecule interacting with acetic acid, as well as to a lower number of acetic acid clusters. The latter behavior can be mainly ascribed to a temperature change in the activation energy of carboxylic groups of acetic acid. These results may be also relevant to better understand the folding mechanism in protein–water solutions.

Introduction

The role of liquid water in the stability and functionality of biological macromolecules is so relevant that the possibility of having living organisms without water is simply axiomatically discarded by modern science.^{1,2} It has already been demonstrated how protein dehydration induces an increase of rigidity and a rise of denaturation temperature, with the consequent loss of physiological functions.^{3,4} Water also influences hydrogen bond (HB) strength and dynamics in biological systems^{2,5–7} and plays a primary role in the protein folding process. The latter seems to be accompanied by the formation of a hydrophobic core with water density around the protein surface higher than the one of bulk water.^{8–10}

Theoretical studies carried out on peptide chains have evidenced how the HB strength in β -sheet structures in aqueous environment results to be three times greater than the one in the gas phase,⁵ thus showing how the presence of water can significantly modify the HB behavior. Moreover, a marked temperature dependence of HB geometry in proteins has also been experimentally observed.¹¹ However, in spite of the remarkable efforts,¹² the role of water in determining the HB behavior of proteins has not yet been completely understood. One of the reasons is the complexity of the analyzed systems, which are also characterized by the coexistence of several HB configurations making it very difficult to isolate the information relative to a given HB species. A possible way to overcome this problem is to study a simple system, in which only the HB species of interest is present or, at least, predominant. This approach has been extensively used in optical Kerr-Effect studies on aqueous systems,¹³ organic solutions,¹⁴ amino acids, and small oligomers¹⁵ and also peptides of different structural complexity.¹⁶

One of the experimental methods used to characterize the HB behavior in water and aqueous systems is Brillouin scattering.^{17–24} In liquids a substantial modification of the dispersion/absorption of longitudinal acoustic (LA) modes can be inferred to the presence of active HB. The effects of HB dynamics on the behavior of longitudinal acoustic modes can be described in terms of structural relaxation processes, which

account for the time decay of density fluctuations correlation function. In the probed frequency region, this dynamics is mainly due to the collective rearrangements of the local structure through intermolecular interactions, which, in the liquid phase, are dominated by the making and breaking of the intermolecular bond network, as observed in previous studies carried out on HB and non-HB systems.^{22–30} Furthermore, the relaxation parameters can be related to damping of LA modes, $\Gamma = \nu_L Q^2 = (\nu_B + (4/3)\nu_S)Q^2$ (ν_L , ν_B , and ν_S being the longitudinal, bulk, and shear kinematic viscosity, respectively), through the relation $\Gamma_L = \sum_i \Delta_i \tau_i$, where τ_i and Δ_i are the characteristic time and strength of the i -th relaxation process. To obtain information on relaxation processes, Brillouin spectra are usually interpreted within the frame of the viscoelastic model. This approach has been widely demonstrated to be reliable in accurately determining the relevant relaxation parameters from the measured spectra,^{23–35} even in the case of aqueous systems of biological interest.¹⁹ Moreover, under certain circumstances from the temperature trend of the Brillouin peak line width, it is possible to directly derive the temperature dependence of the structural relaxation times (τ_i), which, in a first approximation, can be represented with an exponential (Arrhenius) law: i.e., $\tau_i \propto \exp(E_{\text{act},i}/K_B T)$, where K_B is the Boltzmann constant and $E_{\text{act},i}$ is the activation free energy related to the involved HB.^{25–30,34–41} In this context, $E_{\text{act},i}$ can be regarded as the energy required to locally break the HB via, e.g., librational motions.⁴²

Given such grounds, the aim of the present study is to investigate through Inelastic UV Scattering (IUVS) how hydration influences the temperature behavior of HB in simple organic molecules. The studied system is acetic acid (CH_3COOH), which has been chosen for the presence of a carboxylic group, which could be present on the exterior surface of the folded water-soluble proteins. The analysis of the IUVS spectra allowed us to determine the behavior of both sound velocity and activation energy as a function of temperature and acetic acid concentration. The obtained results permitted us to understand how the acetic acid concentration in solution deeply modifies the properties of the HB between water and acetic acid and how such modifications depend on temperature.

* To whom correspondence should be addressed. E-mail: francesco.damico@elettra.trieste.it.

Experimental Section

The experiment was carried out at the IUVS beamline of the Elettra synchrotron facility in Trieste (Italy). Inelastic scattering spectra were acquired in an almost backscattering configuration, exploiting a scattering angle (2θ) of 172° and using a Czerny–Turner analyzer system able to provide an energy resolution of $\Delta E/E \approx 2 \times 10^{-7}$. A detailed description of the experimental apparatus can be found elsewhere.²³ The value of the momentum transfer (Q) is determined by the scattering angle, the wavelength of probing photons (λ), and the refraction index of the sample (n_e); i.e., $Q = 4\pi n_e \sin(\theta)/\lambda$. The value of n_e as a function of concentration and temperature was experimentally measured in the range of interest with an accuracy better than 0.3%, following the procedure reported in ref 43.

The sample was acetic acid (Aldrich) diluted in bidistilled water. IUVS spectra of acetic acid water solutions at three representative n (i.e., $n = 3.2, 4.8$, and 28.5 where n is the ratio between water and acetic acid molecules) were collected as a function of temperature (T) in the $275 \div 365$ K range with T-steps of 5 K to cover the whole liquid phase of the probed sample. Spectra of pure water and pure acetic acid in the same T-range were also measured for comparison. Finally, for $T = 295$ and 355 K, we also collected IUVS spectra as a function of n in the 0 – 80 n -range.

The sample was placed in a 2 mL UV-graded quartz cell positioned in the beamline experimental chamber. The temperature was controlled by means of a close-cycle chiller and a resistive heater kept in thermal contact with the sample cell; the thermal stability was ensured by a PID device. The actual T-value was monitored by a thermocouple, and an overall T-stability better than 0.5 K was found. IUVS spectra, $I(Q, \omega)$, were analyzed through a fitting procedure based on a standard χ^2 minimization. $I(Q, \omega)$ line shape was described by the function

$$I(Q, \omega) = R(\omega) \otimes [A_1 \delta(\omega) + A_2 S(Q, \omega)] + B \quad (1)$$

where $R(\omega)$ is the experimentally determined energy resolution function; $\delta(\omega)$ is a Dirac function accounting for spurious elastic scattering from the experimental apparatus; $S(Q, \omega)$ is the dynamic structure factor; A_1 and A_2 are scaling factors; and B is the background, which was explicitly measured.

Though different relaxations could be in principle associated with different types of HB, it is usually assumed that the relaxation function can be approximated by a single relaxation process.^{23–26,30–41} This assumption is endorsed by the observation that relaxation processes associated with a different kind of HB have very similar time scales (in the picosecond range). Within this assumption, in the framework of the viscoelastic model⁴⁴ $S(Q, \omega)$ can be approximated by the following function (viscous approximation)

$$S(Q, \omega) = \frac{S(Q)}{\pi} \frac{\Omega^2 \Gamma}{[\omega^2 - \Omega^2]^2 + [\omega \Gamma]^2} \quad (2)$$

where the parameters $\Omega^2 = c_s^2 Q^2 + R$ and $\Gamma = \Delta_\alpha \tau_\alpha Q^2 - D$ determine the characteristic frequency and line width of inelastic excitations. Here Δ_α and τ_α are the relaxation strength and time, respectively, while c_s is the adiabatic sound velocity of the solution; finally, R and D are corrective terms of the order of $(\omega \tau_\alpha)^2$. In the data evaluation, we neglected the latter terms since in the probed (ω, T) -range the condition $\omega \tau_\alpha \ll 1$ is essentially

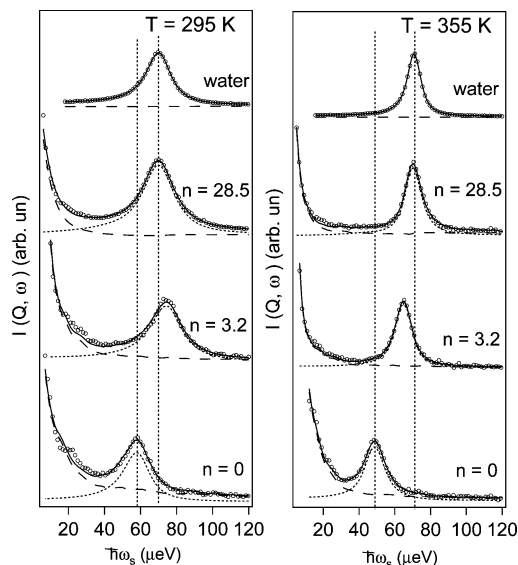


Figure 1. Selection of IUVS spectra from water, acetic acid, and acetic acid–water solutions at different n (i.e., the ratio between water and acetic acid molecules) and T values. Experimental data (dots) are plotted together with the best fit results (full lines). The elastic and inelastic contributions are reported as dashed and dotted lines, respectively. The vertical dotted lines report the peak maximum positions in water and acetic acid.

fulfilled, and consequently, R and D may only lead to a few percent deviations of Ω^2 and Γ with respect to $c_s^2 Q^2$ and $\Delta_\alpha \tau_\alpha Q^2$, respectively.^{20,44} The analysis of such small effects, though potentially interesting, falls beyond the aim of the present work. On the basis of previous results^{20,25,35,45} we assumed that the T-dependence of Δ_α is negligible with respect to the one of τ_α . Therefore, we identify the T-behavior of Γ/Q^2 with the one of τ_α . Moreover, we would like to remark how pH variations on acetic acid solutions have irrelevant effects on $S(Q, \omega)$ because the ionized acetic acid molecules are less than 1% for all the concentrations used in our experiment.

Figure 1 shows selected IUVS spectra of water, acetic acid, and acetic acid–water solutions at different n and T -values. The experimental data are plotted together with the corresponding best fit results, highlighting the correct choice made for the fit function.

Results and Discussion

Figure 2 displays the T-dependence of c_s , as extracted from the fitting procedure, for pure water, pure acetic acid, and selected acetic acid solutions. In the $293 \div 303$ K T-range, the values of c_s are close to the ones found by Gonzalez and co-workers,⁴⁶ confirming the validity of our analysis.

The c_s linear temperature decrease observed for acetic acid is maintained in the whole T-range up to the stoichiometric ratio of ~ 3 . For n -values from 3 to 5 the nearly linear T-trend is preserved with a similar temperature coefficient for $T < 325$ K, while at higher temperatures an odd behavior of c_s with respect to the linear trend can be readily observed. In the following, we indicate such crossover temperature as $T_c = 325 \pm 10$ K. At higher n 's, the T-dependence of sound velocity becomes increasingly similar to that of water.

The first relevant information evidenced by the data reported in Figure 2 is that the departure from the linear behavior of c_s can be observed for n -values larger than ≈ 3 and for temperatures higher than $\approx T_c$. Finally, it is also worth noting that for low temperatures the solutions characterized by n -values in the $3 \div$

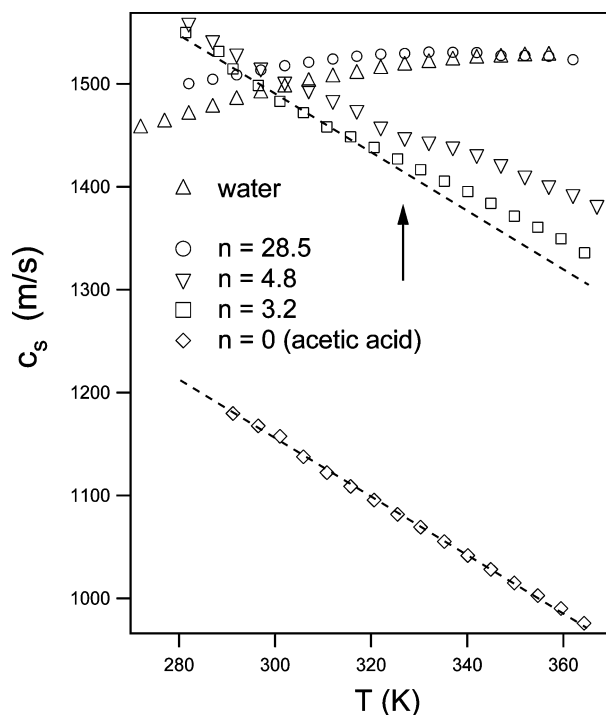


Figure 2. Temperature dependence of sound velocity in water, acetic acid, and acetic acid–water solutions at different n values. The error bars are within the dimensions of the points. The arrow evidences the T_c position.

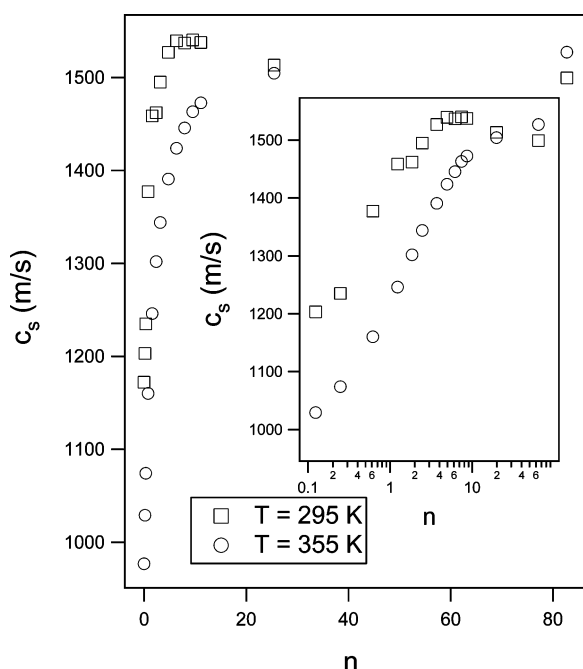


Figure 3. Sound velocity of acetic acid water solutions reported as a function of n for two different temperatures. In the inset, the same graphic is reported with the n axis in logarithmic scale. The error bars are within the dimensions of the points.

5 range present a sound velocity higher than the one of water at the corresponding temperature.

To better understand this phenomenology, in Figure 3 we show the dependence of c_s on n for two T -values (295 and 355 K) above and below T_c . The observed trend of c_s is noteworthy different at the considered temperatures. At 295 K, c_s steeply increases by more than 50% from $n = 0$ to $n = 5$, where the sound velocity reaches its maximum value. On increasing n , c_s

remains close to the maximum value, while for $n > 10$ it slightly decreases up to asymptotically reach the pure water value (i.e., $c_s = 1488$ m/s at 295 K⁴⁷) when acetic acid concentration becomes negligible. At 355 K, the n dependence of c_s is rather different since the initial increase of c_s is smoother and no maximum can be found. As in the previous case, for large n -values c_s reaches the value found for pure water at the corresponding temperature (i.e., $c_s = 1554$ m/s⁴⁷).

The behavior of c_s as a function n and T can be qualitatively explained by analyzing the (n, T) -behavior of the average HB activation energy (E_{act}), as determined by the T -trend of the parameter Γ/Q^2 assuming an Arrhenius T -dependence of relaxation time (at least close to the actual T -value). Figure 4 shows a semilogarithmic plot of Γ/Q^2 vs the inverse temperature for water and acetic acid–water solutions. The straight lines in each single panel represent the Arrhenius trend extracted by fitting the five lowest and highest temperature points. It is rather clear how a single Arrhenius trend cannot describe the data in the entire T -range, especially in the case of acetic acid–water solutions. In the case of water, E_{act} increases at low temperature, up to a value of 13.5 ± 0.2 kJ/mol, while at temperatures just below the boiling point E_{act} decreases down to 8.3 ± 0.6 kJ/mol. These values are in agreement with those reported by other investigators.^{35–37,42,45,48–50} In pure acetic acid instead (Figure 5), a single Arrhenius trend, characterized by an E_{act} value lower than that of water, can be identified within the experimental error ($E_{act} = 5.0 \pm 0.3$ kJ/mol).

At room temperature, pure acetic acid is structured into two dimer species, both of them showing an HB involving the carboxylic groups of the two molecules and with an enthalpy (H_{AA}) of 26.5 and 27.0 kJ/mol.^{51,52} The remaining methyl groups of the dimers can form only weak bonds, thus leading to the observed remarkable decrease of activation energy. On the other hand, the enthalpy of water–water HB (about 20.9 kJ/mol⁵³) is expected to be larger than that of HB between methyl groups of acetic acid dimers and water (about 7.6 kJ/mol⁵⁴). Therefore, the formation of HB between the dimers and the surrounding water molecules is unfavored with respect to the formation of an extended HB network of interconnected water molecules. In this case, the system should be essentially composed by acetic acid dimers not bonded to each other, and consequently, the measured E_{act} value should be similar to the one of water. This picture is consistent with the behavior observed at high temperature (see Figure 4).

To obtain a more clear picture of the T -trend of E_{act} , in Figure 6 (panel A) we show the Arrhenius fits performed on five consecutive T -points of the curves shown in Figure 4. Despite the quite large error bars, the data clearly show a low temperature increase in the E_{act} values with respect to the water one. Moreover, although the large amount of noise does not allow a proper estimation, the T_c value ($\approx 325 \pm 10$ K) empirically determined from the data shown in Figure 2 seems to mark fairly well the border of the T -range where the E_{act} values in the solution are reasonably close to the one of water. Therefore, on increasing n for temperatures higher than T_c , no changes in the E_{act} value can be observed, besides the increase from 5.0 ± 0.3 kJ/mol (pure acetic acid) to 8.0 ± 0.9 kJ/mol (the lowest n -value probed in this work). This trend is more evident by inspecting the panel B of Figure 6, where the values of E_{act} obtained from the 5 lowest and highest T -points reported in Figure 4 are reported.

On the other hand, below T_c , E_{act} increases up to 20.3 ± 0.9 kJ/mol at $n = 28.5$ the (largest n -value probed in this work). Since a further increase in n would bring back the E_{act} value to

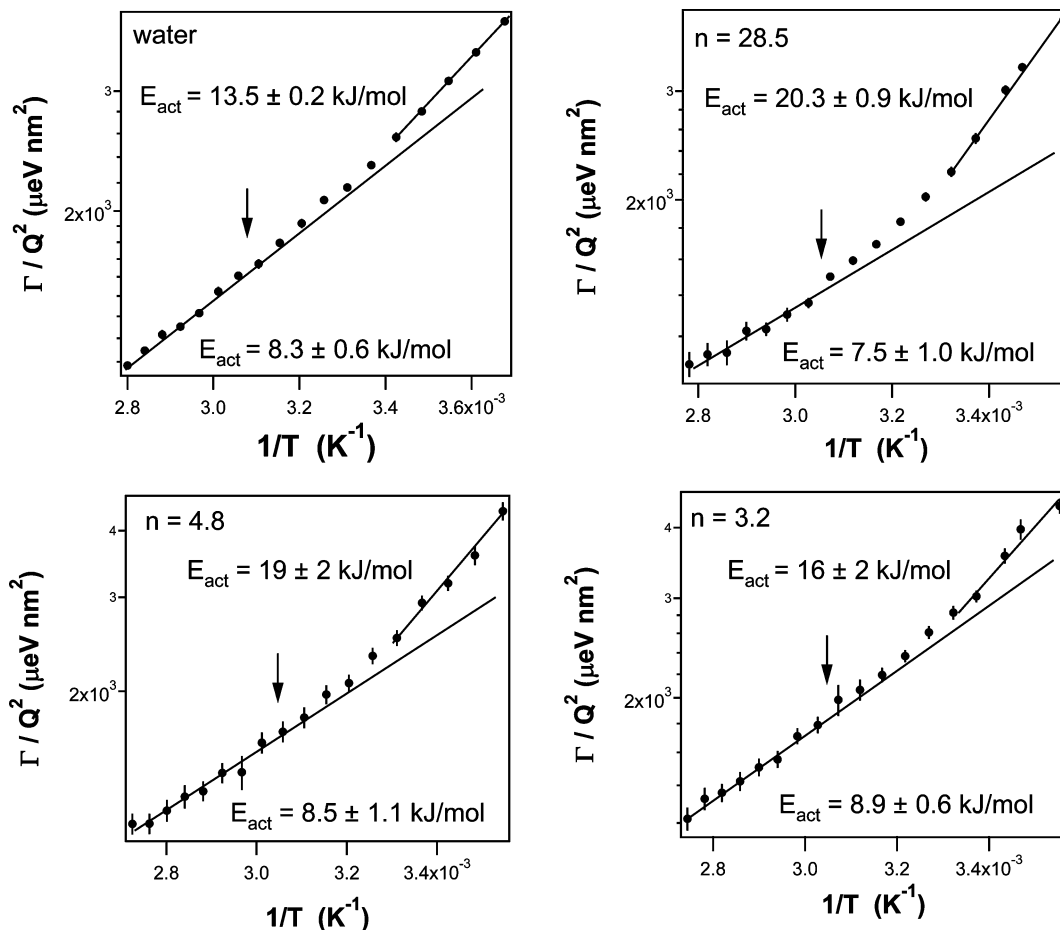


Figure 4. Values of the parameter Γ/Q^2 in water and acetic acid–water solutions at different stoichiometric ratios reported as a function of the inverse temperature. Straight lines are extrapolations performed on the five lowest and highest temperature Γ/Q^2 values using the Arrhenius law: i.e., $\Gamma/Q^2 \propto \exp(E_{\text{act}}/K_B T)$. The obtained values of E_{act} are reported in the individual panels near the corresponding best fit lines. The arrows indicate the T_c position.

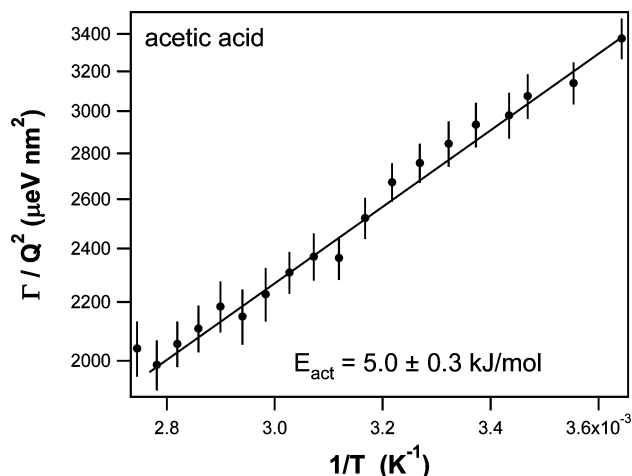


Figure 5. Values of the parameter Γ/Q^2 in acetic acid reported as a function of the inverse temperature. The straight line is the observed Arrhenius trend. The corresponding value of E_{act} is reported.

the water one, the n -trend of E_{act} seems to be qualitatively similar to that of c_s . This behavior can be guessed by looking at the low- T data reported in Figure 6 (panel B). Despite the limited number of data points, we can reasonably suppose the presence of a step n -increase of E_{act} for low- n , followed by a smooth decrease toward the water asymptote. This behavior may indicate that in the $\approx 5 \div 10$ n -range (indicated with an arrow) the system develops energetically favored structures, likely

leading to an overall stiffening of the elastic response and thus qualitatively explaining the low- T n -behavior of c_s reported in Figure 3.

Even though the “average character” of our data does not allow us to discriminate on the nature of such structures nor to identify the roles played by a given HB specie, it is reasonable to suppose that both water and acetic acid molecules are involved. Furthermore, the carboxylic groups of acetic acid may play a relevant role in the E_{act} increase. Therefore, water–acetic acid interactions in the first hydration shell might induce a disruption of the dimers and allow strong bonding between the carboxylic group of acetic acid and water. This mechanism can effectively increase the E_{act} value as far as n is lower than the average number of interacting water molecules per acetic acid molecule. For larger n -values the increase in water content only adds further water–water interactions, with a consequent reduction in the average value of E_{act} toward the value found for water. Within this frame, we can estimate the average number of interacting water molecules to be about 5, which is reasonably lower than the number of water molecules fitting the first hydration shell; however, it is reasonable that only a small fraction of these molecules can effectively form bonds with acetic acid. Another possible effect that can concur to explain the observed phenomenology is the formation of acetic acid clusters in the solution,^{51,52} which lead to an increase in the viscosity.^{55,56} As a consequence, an increase in the value of the parameter Γ/Q^2 (or equivalently τ) is expected. Furthermore, according to the employed definition of E_{act} , if the number of

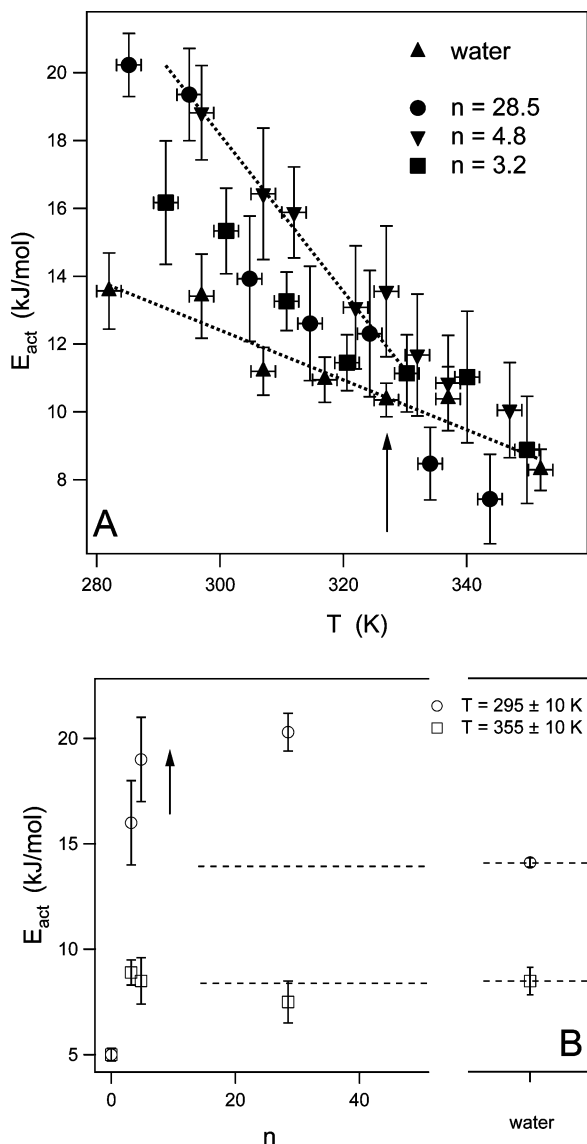


Figure 6. Panel A: Activation energy as a function of temperature at the different indicated n -values, derived from the data in Figure 4 following the procedure described in the text. The arrow indicates the T_c position. Panel B: Activation energies as a function of n for the lower and higher investigated temperatures. The dotted lines report the water activation energies for both the temperatures.

clusters increases at low- T (as usually observed⁵⁷) then an increase in the E_{act} value can be detected. This increase is not necessarily related to the formation of a stronger HB, but rather to a slowing down of the dynamics associated with structural effects. The low- T formation of acetic acid clusters in the solutions with $n > 5 \div 10$ (as observed in ref 51) may turn into an increase of the observed E_{act} value, therefore qualitatively accounting for the smooth n -decrease of E_{act} toward the value found in water.

The disappearance of this phenomenology above T_c may be ascribed to a different entropic contribution for the HB between acetic acid molecules and the ones between water molecules. Indeed, it is commonly accepted that on increasing T the HB network of bulk water loses its marked tetrahedral (low entropy) structure. Therefore, on increasing T it is reasonable to suppose that, on thermodynamic grounds, the water–water HB may become almost equally favored with respect to the acetic acid–acetic acid HB because of the large entropy increase of

the former. If the two HB species have similar activation energies, then the change in n becomes less relevant.

Conclusions

In summary, our experimental data have evidenced how the behavior of acetic acid aqueous solutions presents marked differences below and above a crossover temperature $T_c \approx 325 \pm 10$ K. The observed phenomenology can be ascribed to peculiar acetic acid–water interactions and to the specific acetic acid structure, which allows the formation of stiff HBs between the carboxylic group and the surrounding water molecules, thus leading to an increase of the average HB activation energy below T_c . Moreover, we found a temperature limit (T_c), above which the energy of the involved water–acetic acid HB becomes comparable with the one of HB in bulk water, and consequently, the aforementioned increase of average activation energy is no longer observed.

Here it is worth pointing out how in folded proteins the main HB in a polypeptide chain involves the NH and the C=O groups of the peptide unit.⁵⁸ As a consequence, on the basis of the results of the present work, it is not unrealistic to suppose that a stiffening below a certain crossover temperature may occur also in the HB involved into the protein folding processes. In this context, it is interesting to notice that proteins systems (such as, e.g., lysozyme) usually present a characteristic temperature of about $340 \div 370$ K, above which a defolding process and a consequent loss of biological functionality occurs.^{59,60}

Since the results of the present study deal with a very simple model system, we are too far to establish a reliable similarity between the acetic acid crossover temperature and the lysozyme folding temperature. However, these results indicate that the temperature behavior of E_{act} in simple organic aqueous solutions could be of great relevance in understanding the protein folding process and open the way for further investigations on water–organic systems.

Acknowledgment. C. Masciovecchio acknowledges support from the European Research Council under the European Community Seventh Framework Program (FP7/2007-2013)/ERC IDEAS Contract No. 202804.

References and Notes

- (1) Bellissent-Funel, M. *J. Mol. Liq.* **2000**, *84*, 39–45.
- (2) Mattos, C. *J. Mol. Liq.* **2002**, *27*, 203–208.
- (3) Daidone, I.; Ulmschneider, M.; Di Nola, A.; Amadei, A.; Smith, J. C. *Proc. Natl. Acad. Sci. U.S.A.* **2007**, *104*, 15230–15235.
- (4) Pal, S. K.; Peon, J.; Zewail, A. H. *Proc. Natl. Acad. Sci. U.S.A.* **2002**, *99*, 15297–15302.
- (5) Sheu, S.; Yang, D.; Selzle, H.; Schlag, W. *Proc. Natl. Acad. Sci. U.S.A.* **2003**, *100*, 12683–12687.
- (6) Doruker, P.; Bahar, I. *Biophys. J.* **1997**, *72*, 2445–2456.
- (7) Klotz, I. *Protein Sci.* **1993**, *2*, 1992–1999.
- (8) Cheung, M.; Garcia, A.; Onuchic, J. N. *Proc. Natl. Acad. Sci. U.S.A.* **2002**, *99*, 685–690.
- (9) Svergun, D.; Richard, S.; Kock, M.; Sayers, Z.; Kuprin, S.; Zacca, G. *Proc. Natl. Acad. Sci. U.S.A.* **1998**, *95*, 2267–2272.
- (10) Koizumi, M.; Hirai, H.; Onai, T.; Inoue, K.; Hirai, M. *J. Appl. Crystallogr.* **2007**, *40*, s175–s178.
- (11) Cordier, F.; Grzesiek, S. *J. Mol. Biol.* **2002**, *715*, 739–752.
- (12) Pace, C. *Nat. Struct. Mol. Biol.* **2009**, *16*, 681–682.
- (13) Foggi, P.; Bellini, M.; Kien, D.; Vercuque, I.; Righini, R. *J. Phys. Chem. A* **1997**, *101*, 7029–7035.
- (14) Vigil, S.; Kuzyk, M. *J. Opt. Soc. Am. B* **2001**, *18*, 679–691.
- (15) Shirota, H.; Ushiyama, H. *J. Phys. Chem. B* **2008**, *112*, 13542–13551.
- (16) Giraud, G.; Wynne, K. *J. Am. Chem. Soc.* **2002**, *124*, 12110–12111.
- (17) Sette, F.; Ruocco, G.; Krisch, M.; Masciovecchio, C.; Verbeni, R. *Phys. Scr.* **1996**, *T66*, 48.
- (18) Teixeira, J.; Bellissent-Funel, M. C.; Chen, S. H.; Dorner, B. *Phys. Rev. Lett.* **1985**, *54*, 2681–2683.

- (19) Di Fonzo, S.; Masciovecchio, C.; Bencivenga, F.; Gessini, A.; Fioretto, D.; Comez, L.; Morresi, A.; Gallina, M. E.; De Giacomo, O.; Cesaro, A. *J. Phys. Chem. A* **2007**, *111*, 12577–12583.
- (20) Bencivenga, F.; Cimattorus, A.; Gessini, A.; Izzo, M. G.; Masciovecchio, C. *Philos. Mag.* **2008**, *88*, 4137.
- (21) Masciovecchio, C.; Santucci, S. C.; Gessini, A.; Di Fonzo, S.; Ruocco, G.; Sette, F. *Phys. Rev. Lett.* **2004**, *92*, 255507.
- (22) Ruocco, G.; Sette, F. *J. Phys.: Condens. Matter* **1999**, *11*, R259–R293.
- (23) Masciovecchio, C.; Bencivenga, F.; Gessini, A. *Condens. Matter Phys.* **2008**, *11*, 47–56.
- (24) Cunsolo, A.; Nardone, M. *J. Chem. Phys.* **1996**, *105*, 3911.
- (25) Bencivenga, F.; Cunsolo, A.; Krisch, M.; Monaco, G.; Ruocco, G.; Sette, F. *J. Chem. Phys.* **2009**, *130*, 064501.
- (26) Bencivenga, F.; Cunsolo, A.; Krisch, M.; Monaco, G.; Orsinger, L.; Ruocco, G.; Sette, F.; Vispa, A. *Phys. Rev. Lett.* **2007**, *98*, 085501.
- (27) Angelini, R.; Giura, P.; Fioretto, D.; Monaco, G.; Ruocco, G.; Sette, F. *Phys. Rev. B* **2004**, *70*, 224302.
- (28) Giura, P.; Angelini, R.; Datchi, F.; Ruocco, G.; Sette, F. *J. Chem. Phys.* **2007**, *127*, 084508.
- (29) Scopigno, T.; Ruocco, G.; Sette, F. *Rev. Mod. Phys.* **2005**, *77*, 881.
- (30) Giugni, A.; Cunsolo, A. *J. Phys.: Condens. Matter* **2006**, *18*, 889.
- (31) Monaco, G.; Fioretto, D.; Masciovecchio, C.; Ruocco, G.; Sette, F. *Phys. Rev. Lett.* **1999**, *82*, 1776.
- (32) Cunsolo, A.; Pratesi, G.; Verbeni, R.; Colonnese, D.; Masciovecchio, C.; Monaco, G.; Ruocco, G.; Sette, F. *J. Chem. Phys.* **2001**, *114*, 2259.
- (33) Fioretto, D.; Comez, L.; Socino, G.; Verdini, L.; Corezzi, S.; Rolla, P. A. *Phys. Rev. E* **1999**, *59*, 1899.
- (34) Bencivenga, F.; Cunsolo, A.; Krisch, M.; Monaco, G.; Ruocco, G.; Sette, F. *Europhys. Lett.* **2006**, *75*, 70.
- (35) Bencivenga, F.; Cunsolo, A.; Krisch, M.; Monaco, G.; Ruocco, G.; Sette, F. *Phys. Rev. E* **2007**, *75*, 051202.
- (36) Danninger, W.; Zundel, G. *J. Chem. Phys.* **1981**, *74*, 2769–2777.
- (37) Montrose, C.; Bucaro, J.; Coakley, J.; Litovitz, T. *J. Chem. Phys.* **1974**, *60*, 5025–5029.
- (38) Turton, D. A.; Wynne, K. *J. Chem. Phys.* **2008**, *128*, 154516.
- (39) Edige, M. D.; Angell, C. A.; Nagel, S. R. *J. Phys. Chem.* **1996**, *100*, 13200.
- (40) Kanaya, T.; Kaji, K.; Inoue, K. *Macromolecules* **1991**, *24*, 1826.
- (41) Angell, C. A. *J. Non-Cryst. Solids* **1991**, *13*, 131–133.
- (42) Starr, F.; Nielsen, J.; Stanley, H. *Phys. Rev. E* **2000**, *62*, 579–587.
- (43) Chandra, B.; Bhaiya, S. *Am. J. Phys.* **1983**, *51*, 160–161.
- (44) Boon, J.; Yip, S. *Molecular Hydrodynamics*; McGraw Hill: New York, 1980.
- (45) Monaco, G.; Cunsolo, A.; Ruocco, G.; Sette, F. *Phys. Rev. E* **1999**, *60*, 5505.
- (46) Gonzalez, B.; Domynguez, A.; Tojo, J. *J. Chem. Eng. Data* **2004**, *49*, 1590–1596.
- (47) Wagner, W.; Pruss, A. *J. Phys. Chem. Ref. Data* **2002**, *31*, 387.
- (48) Slie, W. M.; Donfor, A. R.; Litovitz, T. A. *J. Chem. Phys.* **1966**, *44*, 3712.
- (49) Luzar, A. *J. Chem. Phys.* **2000**, *113*, 10663.
- (50) Chen, S. H.; Teixeira, J. *Adv. Chem. Phys.* **1986**, *64*, 1.
- (51) Nishi, N.; Nakabayashi, T.; Kosugi, K. *J. Phys. Chem. A* **1999**, *103*, 10851–10858.
- (52) Crupi, V.; Magazu, S.; Maisano, G.; Majolino, D.; Migliardo, P.; Musolino, A. M. *J. Mol. Struct.* **1996**, *381*, 219–226.
- (53) Feyereisen, M. W.; Feller, D.; Dixon, D. *J. Phys. Chem.* **1996**, *100*, 2993.
- (54) Li, Q.; An, X.; Luan, F.; Li, W.; Gong, B.; Cheng, J. *J. Phys. Chem. A* **2008**, *112*, 3985–3990.
- (55) Omta, A. W.; Kropman, M. F.; Woutersen, S.; Bakker, H. J. *Science* **2003**, *301*, 347–349.
- (56) Turton, D. A.; Hunger, J.; Heftner, G.; Buchner, R.; Wynne, K. *J. Chem. Phys.* **2008**, *128*, 161102.
- (57) Goncharuk, V. V.; Orekhova, E. A.; Malyarenko, V. V. *J. Water Chem. Technol.* **2008**, *30*, 80–84.
- (58) Baker, E. N.; Hubbard, R. E. *Prog. Biophys. Mol. Biol.* **1984**, *44*, 97–179.
- (59) Lai, B.; Cao, A.; Lai, L. *Biochem. Biophys. Acta* **2000**, *1543*, 115–122.
- (60) Hirai, M.; Koizumi, M.; Hayakawa, T.; Takahashi, H.; Abe, S.; Hirai, H.; Miura, K.; Inoue, K. *Biochemistry* **2004**, *43*, 9036–9049.

JP103730S